

# Driver Status Monitoring Systems for Smart Vehicles Using Physiological Sensors

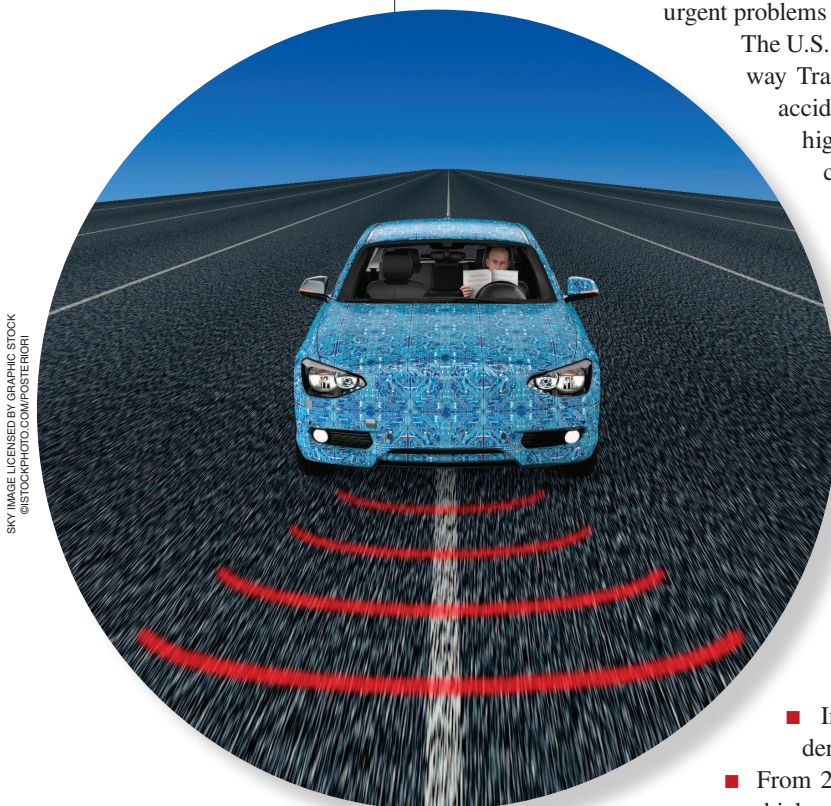
*A safety enhancement system from automobile manufacturers*

**A**utomobiles provide a convenient form of transportation, and the number of automobiles in the world has been increasing rapidly, from 193 million in 1970 to more than 796 million in recent years [1]. However, automobiles have created a number of serious problems, such as accidents, traffic congestion, and air pollution, among which traffic accidents are one of the most serious and urgent problems threatening the safety of automobile users.

The U.S. Department of Transportation National Highway Traffic Safety Administration found that traffic accidents are mostly caused by drivers' inattention, high-speed driving, drunken driving, misperception, decision errors, and driver incapacitation (e.g., falling asleep or having a heart attack while driving). Among these causes, drunken driving and driver incapacitation account for about 25% of total traffic accidents [2]. In 2014, the American Automobile Association Foundation for Traffic Safety in the United States reported that an average of 328,000 traffic accidents annually involve a drowsy driver [3]. In Europe, 20–25% of total traffic accidents were due to drowsy drivers [4]:

- In France in 2011, there were 3,970 fatal accidents on the road, in which 732 cases occurred on straight roads; 85% of these accidents were due to drowsy drivers [4].
- In Germany, 25% of all fatal road traffic accidents were caused by drowsy drivers [4].
- From 2006 to 2010, in Finland, 17% of fatal motor vehicle accidents were related to fatigued drivers; they were responsible for 18% of deaths on the road [4].

Driver status monitoring (DSM) systems have emerged as an innovative technology to prevent traffic accidents from driver incapacitation. In recent developments of DSM systems, medical technologies used for patient diagnosis, including those utilizing electrocardiogram (ECG) and photoplethysmogram (PPG), are considered for the acquisition of driver's physiological signals, which is an effective approach that should be given a special attention.



SKY IMAGE LICENSED BY GRAPHIC STOCK  
©ISTOCKPHOTO.COM/POSTERIORI

## Overview

To reduce the occurrence of serious traffic accidents caused by driver incapacitation due to fatigue and drowsiness, and to protect drivers from fatal accidents, increasing attention is being paid to DSM systems equipped with vision sensors, steering angle sensors (SASs), and physiological sensors. These types of DSM systems has been developed mostly by major automobile manufacturers such as Ford, Toyota, BMW, among others, since the early 2000s [5], and some important technologies are already commercialized or considered for smart vehicles. This article introduces the overall design of DSM systems, as applied to smart vehicles, being developed by the major automobile manufacturers. In particular, we focus on DSM systems utilizing physiological signals such as ECG and PPG, rather than the conventional DSM systems using vision sensors or SAS.

The section “Signal Processing Algorithms for DSM Systems Using Physiological Signals” introduces the signal processing techniques and noise reduction algorithms that are tested and used by the automobile manufacturers for the acquisition and enhancement of physiological signals in noise to extract the parameters related to the driver’s status. Electromagnetic compatibility (EMC) issues that need to be addressed for the application of DSM technologies to actual smart vehicles are introduced briefly in the section “EMC Issues in DSM Systems Using Physiological Signals.” The purpose of this article is to present a guideline for the design of DSM systems for readers who would like to develop the system for commercialization, by introducing the performance of DSM systems as obtained through actual vehicle tests.

## Various DSM technologies

In general, DSM systems utilize various sensors to measure the steering angle, ECG, and PPG to monitor the driver’s status and analyze driver’s physiological signals and movements in the vehicle. The conventional DSM systems are equipped with a camera [charge-coupled device (CCD), infrared (IR), stereo, etc.] installed on the steering column and/or infrared-light emitting diodes (IR-LEDs) mounted inside vehicles so that the system can measure the driver’s eye blink rate, head location, and the driver’s facial direction to detect the driver’s status. Because the detection and recognition performance of the conventional DSM systems largely depend on image and vision processing algorithms, the conventional DSM systems require computationally expensive vision processing algorithms [5], [6], in general.

Some automobile manufacturers have developed DSM systems using driver’s driving patterns so that the performance of the system can be more reliable [4]. In these systems, once the driver’s driving patterns are obtained from a precise SAS, the patterns are stored in the in-vehicle database (DB) and used to estimate the driver’s status by comparing vehicle’s current movements with the DB. However, since a driver’s driving pattern

often depends on the driver’s intention (e.g., driver’s intentional eye blinking does not indicate a driver’s driving pattern), it requires additional information to increase the accuracy in the driver’s status detection [5], [6].

Recently, physiological signals such as ECG and PPG have been used in DSM systems, where the level of detection accuracy is greater when compared to the DSM systems using vision sensors or driving patterns, because the physiological signals are highly correlated to the driver’s physical status [7], [8]. Table 1 shows the features of DSM systems developed by major automobile manufacturers.

## Signal processing algorithms for DSM systems using physiological signals

As mentioned in the section “Various Driver Status Monitoring Technologies,” the conventional DSM systems may not be able to detect a driver’s abnormal status correctly; for example, when a driver’s eye blinking and reckless driving are intentional. Therefore, there has been a strong demand for new DSM technologies [22], and among the new technologies introduced, DSM systems using driver’s physiological signals have gained increasing attention. In general, physiological signals are classified into ECG and PPG, which are measured from the driver’s heart rate and pulse, respectively. In recent realizations of DSM systems using physiological signals, ECGs are more reliable in noisy in-vehicle environments. Therefore, this section focuses on DSM systems that utilize ECG and PPG for the primary and secondary observations, respectively. In addition, we will later introduce DSM algorithms used in the DSM systems.

## Overall process of DSM systems using physiological signals

A single cycle of the ECG consists of a P signal, a QRS complex, and a T signal (refer to [23, Fig. 1]). Among them, the QRS complex has a relatively higher amplitude and signal-to-noise ratio (SNR) in comparison with the P and T signals, so it is utilized to monitor driver’s physical status. On the other hand, a single cycle of the PPG is composed of systolic and diastolic peaks [24]. Since the systolic peak has a relatively higher amplitude than the diastolic peak, it is used to detect the driver’s physical status.

In the system configuration, DSM systems using physiological signals consist of a physiological signal measurement block and a DSM algorithm. The physiological signal measurement block employs an analog signal processing technique for ECG acquisition, which is classified into a contact-based ECG acquisition technique that obtains ECG through the driver’s two hands on the steering wheel, and a noncontact-based ECG acquisition technique that acquires ECG through a capacitive connection between the driver and the electrodes on the driver’s seat. The contact-based ECG acquisition technique uses two electrodes installed on the steering wheel to have

direct contact to both of the driver's hands. Since at least three measurement points on the body, i.e., two points on the left and right sides of the heart and a ground point, are necessary to stably measure the ECG, the analog signal processing technique utilizes the ground point on the analog circuit as a virtual ground point. The noncontact-based ECG acquisition technique uses pairs of electrodes for a stable ECG measurement, where a pair of electrodes is considered as a single channel to measure the ECG. The noncontact-based ECG acquisition technique improves the quality and sensitivity of the ECG measurement by utilizing simultaneous measurements obtained from multiple channels. In practice, both the contact-based and noncontact-based ECG acquisition techniques utilize an instrumental amplifier (INA) that has a high common mode rejection ratio (CMRR) (generally 80~120 dB) to clearly acquire and amplify weak ECG in mV units under very noisy environments. On the other hand, the PPG is measured by illuminating a point on the hand with a light and detecting the reflecting light; a photo detector is used to detect reflected lights from the tissue, blood vessels, and bone.

The analog signal processing technique for PPG (in other words, the contact-based PPG acquisition technique) uses

a nanometer green LED and current to voltage converter to acquire and amplify the weak PPG. In practice, high-pass filter (HPF), low-pass filter (LPF), and notch filter are employed to reduce the amplified noise and to enhance the acquired ECG and PPG [22].

The DSM algorithm consists of three functions performing QRS detection, signal enhancement, and driver status analysis. The QRS detection function extracts the QRS complex from ECG. Generally, threshold-based detection is widely used for easy implementation and low computational complexity, and depending on the threshold determination, there are fixed threshold (FT) and adaptive threshold

(AT) methods [22] used in practice. The FT method can be used effectively in a stationary ECG, however, the AT method can improve the accuracy of the QRS complex detection by setting thresholds adaptively, even though it may not provide a universal solution. In addition, there are other methods used for the QRS detection, for example, based on the neural networks and hidden Markov models, but due to disadvantages such as implementation difficulty and high computational cost, other methods are used only in medical applications that require high reliability.

**In the system configuration, DSM systems using physiological signals consist of a physiological signal measurement block and a DSM algorithm.**

**Table 1. Classification of various DSM techniques.**

Manufacturer	Development Status	Classification	Method
BMW [9], [10]	R&D	ECG	Monitoring heart rate using a steering wheel with a skin-resistance sensor
Mercedes Benz [11], [12]	Commercialized	Steering pattern	Analyzing of driving pattern with 70 parameters by a SAS and other drivers' behaviors, such as audio/air conditioner/window switch use
	R&D	ECG, PPG	Fusing PPGs and ECGs
Volkswagen [13]	Commercialized	Steering pattern	Monitoring counter-steering patterns
	R&D	Vision	Tracking head position, eye and face with a camera, light source, and image processor
Volvo [14]	Commercialized	Steering pattern	Monitoring steering patterns near the lane using a front camera and an SAS
	R&D	Vision	Comparing the threshold and current value by monitoring gaze, eyelids, eye blink rate, and head (or face) angle using a dashboard-mounted IR sensor and camera
Ford [15], [16]	R&D	ECG	Monitoring heart rate using noncontact-based ECG sensor implemented in a car seat
Toyota and Denso [8], [17]–[19]	Commercialized	Vision	Monitoring gaze, eyelids, eye blink rate, and head position using a dashboard-mounted IR-LED and a complementary metal–oxide–semiconductor camera
	R&D	ECG, PPG	Monitoring ECG and PPG using a steering wheel with different electrodes and 525 nanometer green LEDs
Denso [20]	R&D	ECG	Monitoring heart rate using noncontact-based ECG sensor implemented in a car seat
Nissan [21]	Commercialized	Steering pattern	Monitoring the constructed baseline of a given driving path with the driver's steering patterns using a SAS
	R&D	EEG	Predicting the driver's next driving actions beyond estimating the state and cognition of the driver



The signal enhancement function distinguishes the QRS complex from a distorted QRS complex by variability, abnormalities, low SNR, and artifacts [22]. This function makes use of the amplitude and slope of the R-peak as characteristic features, and a combination of Hilbert transformation (HT), mathematical morphology (MM), empirical mode decomposition (EMD), and filter banks (FBs) can be used; HT is used to extract the signal envelope, which is a characteristic feature of the ECG, MM shows excellent performance in reducing the impact of motion artifacts and line drifts, and EMD and FBs convert the QRS signal into a frequency domain and decompose the entire spectrum into subband spectrum.

The driver status analysis function measures the heartbeat interval (the interval between R-peaks, also known as the *RR interval*). The heart rate variability (HRV) technique [7] uses variations of the measured RR intervals to analyze a driver's autonomic nervous activity in either the time or frequency domain [23]. The analysis in the time domain utilizes mean RR (seconds), standard deviation of the RR interval (SDNN) (milliseconds), mean heart rate (HR) (beats/minute), standard deviation of the HR (Std RR) (milliseconds), and the root mean square of successive heartbeat interval differences (RMSSDs) (milliseconds) to estimate the effect of the autonomic nervous system on HR [7]. On the other hand, the frequency-domain analysis is classified into parametric and nonparametric methods [7]. The parametric and nonparametric methods estimate the power spectrum density (PSD) by means of the autoregressive (AR) model and fast Fourier transform (FFT) [25], respectively. The parametric method computes the power in low frequency (LF) and that in high frequency (HF) ( $LF_{AR}[\text{ms}^2]$ ,  $HF_{AR}[\text{ms}^2]$ ), and the percentage of the power in the low- and high-frequency segments ( $LF_{AR}[\%]$  and  $HF_{AR}[\%]$ , respectively) in the parameterized FFT spectrum. Similarly, the nonparametric method estimates the power in low and high frequencies ( $LF_{FFT}[\text{ms}^2]$ ,  $HF_{FFT}[\text{ms}^2]$ ), and the percentage of the power in low- and high-frequency segments ( $LF_{FFT}[\%]$ ,  $HF_{FFT}[\%]$ ) in the FFT spectrum [7]. The frequency ranges of 0.04–0.15 Hz and 0.15–0.4 Hz are used for low- and high-frequency segments, respectively.

Slow-acting sympathetic activity may increase the HR, while fast-acting parasympathetic activity decreases the HR. A sympathetic activity influences the power in both low and high frequencies, whereas a parasympathetic activity makes an effect on the power only in high frequency. The balance between the effects of the sympathetic and parasympathetic activities is referred to as the *sympathovagal balance*, which can be measured by the ratio of powers in LF to that in HF [23]. It is found that when the sympathovagal balance changes to increase a sympathetic activity, the RR interval increases, and the driver status analysis function detects that the driver workload decreases (driver falls asleep). On the other hand, when the sympathovagal

balance changes to increase a parasympathetic activity, the RR interval decreases and the driver workload increases (driver wakes up).

### Analog signal processing for DSM systems using physiological signals

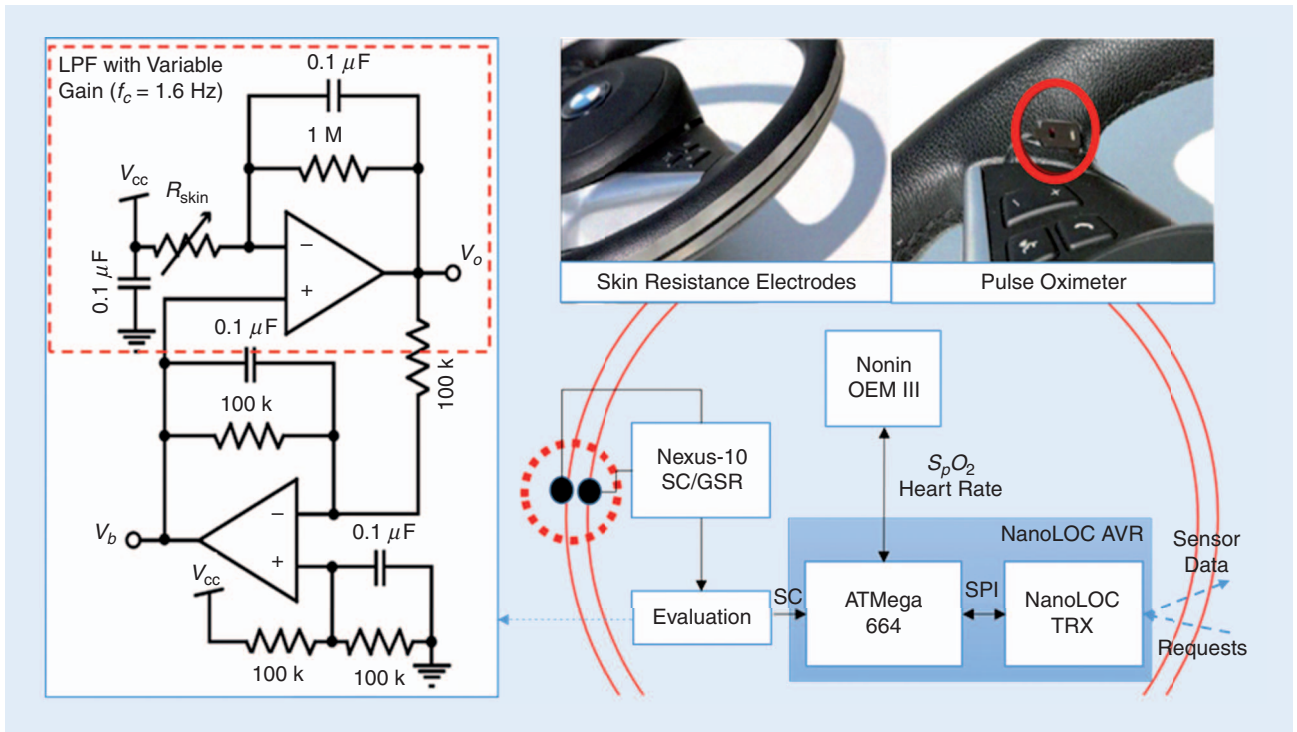
Automobile manufacturers such as Toyota, Ford, BMW, and Daimler AG have been developing DSM systems using the ECG and PPG of the driver since the late 2000s [6], and some of these DSM systems are applied to actual vehicles. In 2010, BMW jointly developed a steering wheel with Technische Universitaet Muenchen as part of the Fit4Age Project. The developed steering wheel features contact-based signal acquisition using a strip-type skin-resistance sensor and a punctiform-type reflective pulse oximetry PPG sensor, which are installed in the BMW 730d [10]. In the system shown in

Figure 1, two conductive strip electrodes are attached all around the steering wheel to measure the driver's skin resistance. Because the resistance acquired from the driver's skin depends on how the driver holds the steering wheel, an electrodermal activity (EDA) circuit [26] that applies an automatic bias control using two operational amplifiers is applied to increase the

dynamic range of sensors [10]. A real driving test of a BMW 730d equipped with the developed steering wheel is conducted by 21 test drivers of average age 65. These participants drove the vehicle three times during 10 minutes on a 16-km long preselected route (highways, state roads, and urban areas) to evaluate the actual performance of the developed steering wheel [9]. From the driving test, it is found that approximately 81% of the meaningful measurements of skin resistance were obtained from the strip-type sensor, while 44% of the valid measurements of PPG were observed from the punctiform-type sensor. One study [9] reported that employing a strip-type sensor is suitable for commercializing the developed steering wheel by BMW.

From 2008 to 2011, Denso, in collaboration with Toyota and Nippon Medical University, developed a special steering wheel that can measure (acquire) ECG and PPG [17]–[19]. For ECG acquisition, positive and negative electrodes are attached to the right and left sides of the steering wheel, respectively, and chrome-coated metal electrodes with high input impedance (90,000  $\Omega$ ) are used. From the steering wheel, 1–5 mV ECG is measured through the electrodes and amplified about 1,700 times. For PPG acquisition, a 525-nm green LED is attached on the steering wheel, which is widely used to reduce the surface reflection from the skin. The baseline wander, considered as an artifact caused by perspiration, respiration, body movements, and unstable contact with electrodes, is minimized after the acquired ECG and PPG pass through an HPF ( $f_c = 0.3$  Hz for both ECG and PPG) [18]. Similarly, noise is minimized using an LPF ( $f_c = 35$  Hz for ECG and  $f_c = 30$  Hz for PPG), and then, the measured ECG and PPG are digitalized by an analog-digital converter (ADC)

**Slow-acting sympathetic activity may increase the HR, while fast-acting parasympathetic activity decreases the HR.**



**FIGURE 1.** A contact-based physiological signal measurement technique developed by BMW [10], [26].

at a sampling rate of 100 Hz and a resolution of 10 bits, as shown in Figure 2. Since the contact area between the steering wheel and the driver's hands varies irregularly while turning the steering wheel on a curvy road and driving on an uneven road, the acquired ECG and PPG include a large amount of noise. Therefore, SNR improvement is required when ECG and PPG are measured through the contact on the steering wheel in real driving environments. From the real driving tests on several roads, Denso found that the SNRs of ECG and PPG required more than 10 dB and 40 dB, respectively, to extract clear ECG and PPG. It is demonstrated that the SNR of PPG varies from 34 dB (stationary vehicle) to 15 dB (driving vehicle) during real driving tests at the speed of 80 km/hour and under acceleration of  $0.65 \text{ m/s}^2$ . The SNR of PPG can be deteriorated by 19 dB, while the SNR of ECG is degraded by 8 dB under the identical driving test condition [18]. To improve the SNR of PPG by enhancing the physical contact, a spring was mounted under the bottom of the PPG sensor to maintain a constant contact area between the driver's hands and the PPG sensor [18]. In addition, an ECG-triggered ensemble-averaging (ETEA) signal processing technique [18] that utilizes the peak detection with the ECG is applied to improve the SNR. As a result, Denso found that the SNR of PPG could be improved by 27 dB from 15 dB (without a spring and an ETEA) to 42 dB (with both a spring and an ETEA) during real driving tests at the speed of 80 km/hour and under acceleration of  $0.65 \text{ m/s}^2$ .

**ECG cannot be acquired with one hand because the contact-based technique requires that at least both hands are continuously in contact with the steering wheel.**

In practice, ECG cannot be acquired with one hand because the contact-based technique requires that at least both hands are continuously in contact with the steering wheel. Therefore, some automobile manufacturers attempt to overcome this problem by developing noncontact-based techniques.

In 2013, Denso [20] developed a noncontact-based ECG acquisition technique utilizing a capacitance coupling between the driver and electrodes installed under the seat cover of the backrest. Denso's noncontact-based ECG acquisition technique utilizes the impedance, generated on the seat cover and the driver's clothing, which varies depending on the driver's physique, seating posture, and the type of clothing. Denso measured the impedance of the leather seat, T-shirt, shirt, and jacket and developed an equivalent circuit of the measured impedance of each clothing in the form of parallel RC circuit. The resistance ( $R$ ) components of the input impedances  $Z_1$  and  $Z_2$  have large values (in units of tera-ohms) in the sensor head [20], where  $Z_1$  and  $Z_2$  represent the combined impedance of the seat cover and clothing. The value of the circuit input resistance  $R_I$  is set to  $1 \text{ G}\Omega$  to prevent a gain reduction due to a resistance-based voltage division and to maintain a dc bias value. In addition, the driven right leg (DRL) [27] circuit is applied to provide a feedback to the driver and to reduce the effect of static electricity resulting from the common mode noise. In [20], it is shown that the noncontact-based ECG acquisition technique achieves a target CMRR of

120 dB, and a higher CMRR is obtained by providing feedback from an electrode on the steering wheel gripped by the driver's hands, which is illustrated in Figure 3. The noise in the ECG is minimized by HPF ( $f_c = 7$  Hz) and LPF ( $f_c = 70$  Hz), and digitized by an ADC with a sampling rate of 1 kHz. The values of  $Z_1$  and  $Z_2$  will be close (balanced) to each other when the driver's back is in a good contact with the seat. However, if  $Z_1$  and  $Z_2$  lose a balanced state due to the driver's motion, the CMRR may decrease. Therefore, a multichannel noncontact-based ECG acquisition technique using a multiplexer is developed to achieve the CMRR value of larger than 120 dB. The performance of Denso's noncontact-based ECG acquisition technique is verified in a series of driving tests on straight roads and curves at a speed of about 70 km/hour [20]. From the real driving tests, the SNR (the ratio of the R-peak in the QRS complex to the baseline noise) of the measured ECG in cruise control is found to be 6.4 dB, and that under acceleration and deceleration is 5.9 dB.

Ford developed a noncontact-based ECG technique employing six insulated electrodes (tin-coated copper plates of  $8 \text{ cm} \times 5 \text{ cm}$  in size) as ECG measurement sensors attached on the backrest of the seat [15], [16]. The technique was jointly developed with Aachen University in Germany and the Philips Chair for Medical Information Technology in 2011, and is applied to Ford's S-Max [16]. Ford utilizes the capacitive ECG (cECG) method [15] to obtain ECG measurements, even when the driver wears thick clothing. The impedance depends on the distance between the driver and insulated electrodes, which varies irregularly due to the driver's motion. In the technique, the impedance must be kept high, therefore, the active electrode technique [28] is applied to maintain a high impedance. Moreover, since the noncontact-based ECG acquisition technique is sensitive to noise; an active shielding technique [29] is needed to reduce the effect of noise. In the equivalent circuit of the active electrode, as depicted in Figure 4 [15], the overall coupling impedance  $Z_{\text{couple}}$  between the driver and the insulated electrode can be computed using  $Z_{\text{couple}} = 1 / ((1/R_{\text{cloth}}) + j\omega C_{\text{cloth}}) + 1 / ((1/R_{\text{ins}}) + j\omega C_{\text{ins}})$ , where,  $R_{\text{ins}}$  and  $R_{\text{cloth}}$  are the resistance of the electrode insulation and the driver's clothing, respectively, while  $C_{\text{cloth}}$  and  $C_{\text{ins}}$  represent the capacitive behavior of the overall contact impedance [15]. For a sufficient voltage drop at the input of the active electrode, a high-input impedance  $Z_B$  is required in the front end of the operational amplifier. The impedances  $Z_{\text{couple}}$  and  $Z_B$  perform high-pass filtering, therefore, noise components at the low frequencies of the measured ECG are removed sufficiently. However, when using the cECG method, static charges stored in the coupling capacitance and on the clothing should be removed, for which the bias resistance ( $R_{\text{Bias}}$ ) is connected to  $Z_B$  in parallel. Since  $Z_B$  is large, the overall amplifier input impedance ( $Z_E$ ) becomes  $Z_E = (R_{\text{bias}} Z_B / R_{\text{bias}} + Z_B) \cong R_{\text{Bias}}$  [15]. Since coupled power-line interference occurring from electrodes exists in the ECG measurements [30], an INA with CMRR of about 115 dB is applied to remove the interference. In addition, LPF is used to remove the harmonics of the interference that is 50 Hz or

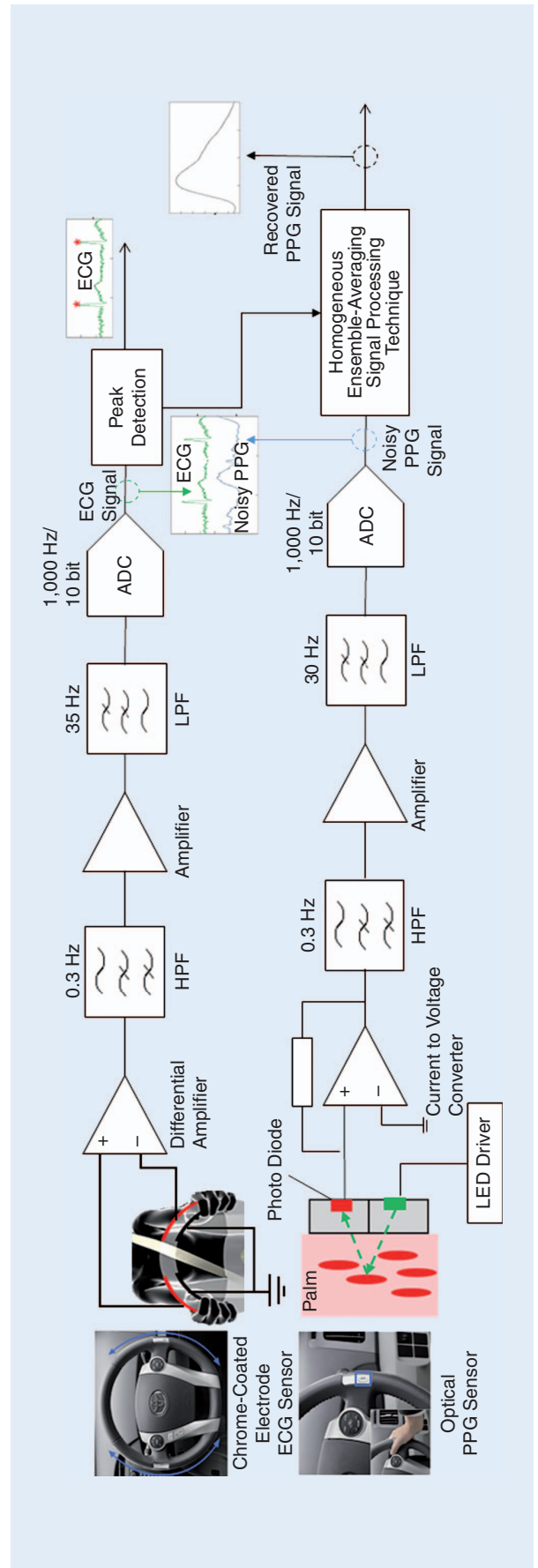


**FIGURE 2.** Analog signal processing for contact-based ECG and PPG acquisition by Toyota and Denso [18].



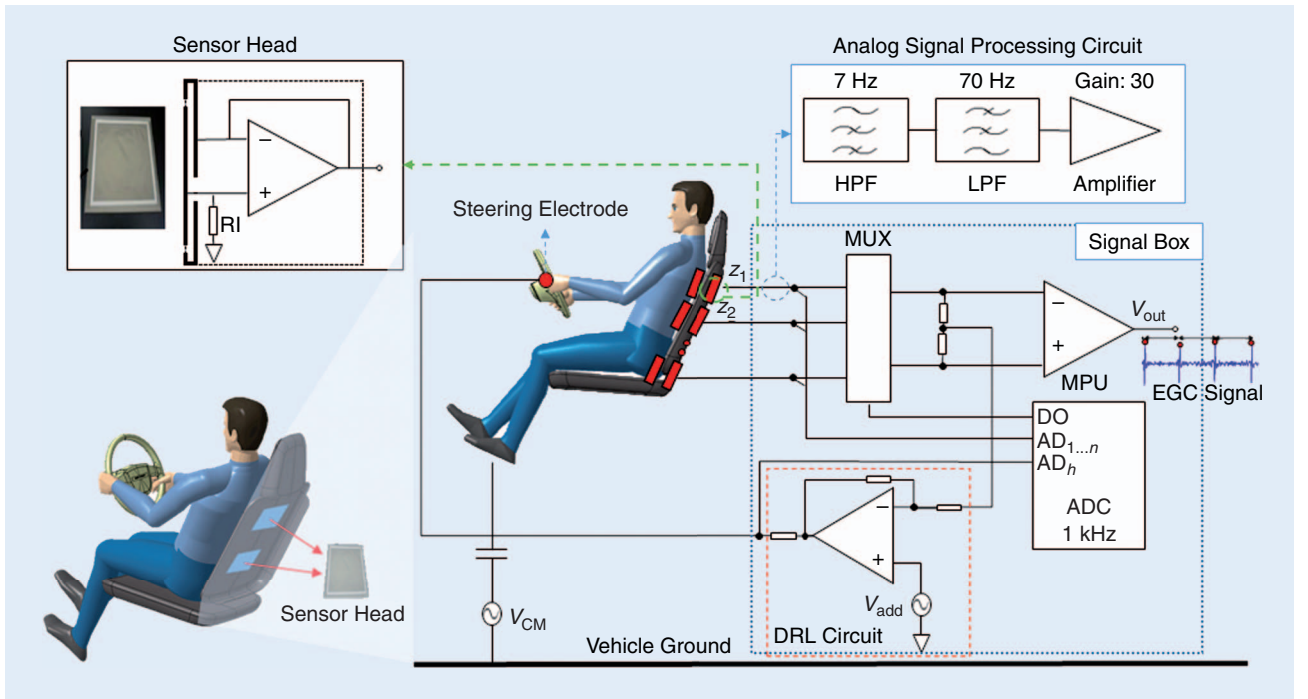


FIGURE 3. Analog signal processing for noncontact-based ECG acquisition by Denso [20].

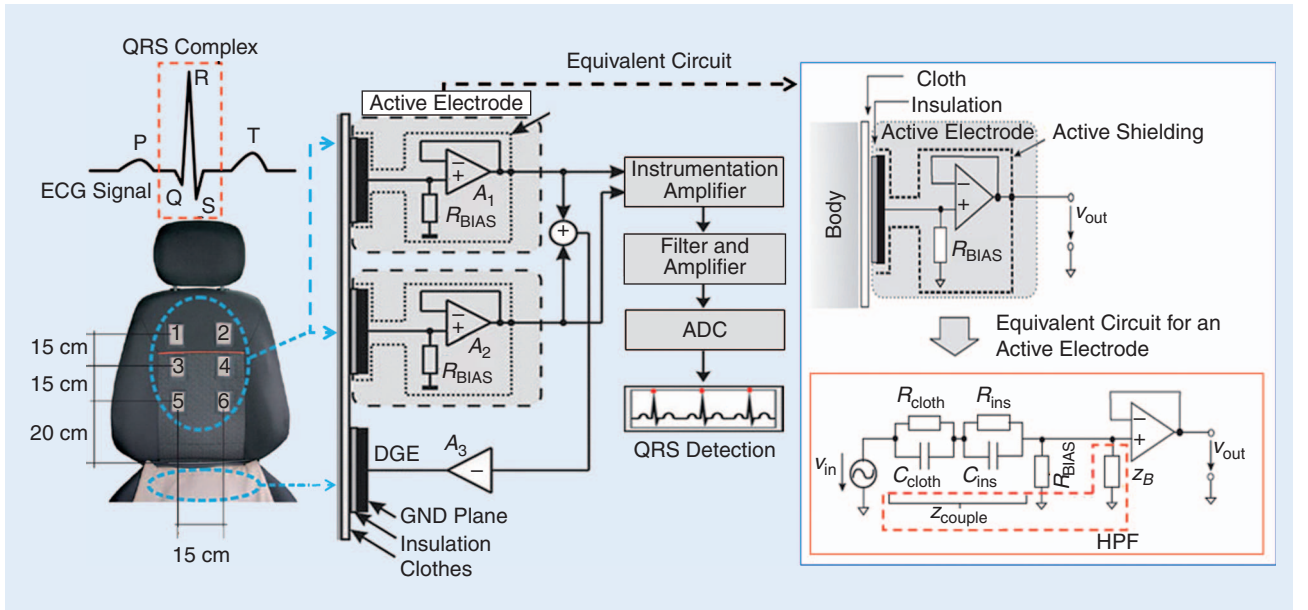


FIGURE 4. Analog signal processing for noncontact-based ECG acquisition by Ford [15], [16].

higher, and other noise components at a high frequency (typically  $>100$  Hz). A notch filter ( $f_c = 50$  Hz) is also used to further suppress noise components in the LPF output, while a HPF ( $f_c = 0.3$  Hz) is employed to remove the dc noise component and to minimize the baseline drift. In [30], the driven ground electrode (DGE) method is used to reduce the interference on the cECG measurements additionally. Ford performed real driving tests with five subjects. The percentage of time ( $T_{icp}$ ), during which at least four consecutive RR intervals is found

in the ECG measurements, is calculated; as a result, it is demonstrated that  $T_{icp}$  in the highway driving ( $T_{icp} = 65\% \sim 98\%$ ) is much higher than that in the city driving ( $T_{icp} = 6\% \sim 63\%$ ) [16]. This proves that Ford's noncontact ECG acquisition technique is suitable to measure the ECG while driving on the highway.

Daimler AG [10], [31] utilizes both contact-based and noncontact-based ECG acquisition techniques. As shown in Figure 5, five electrodes, made of brass, are attached

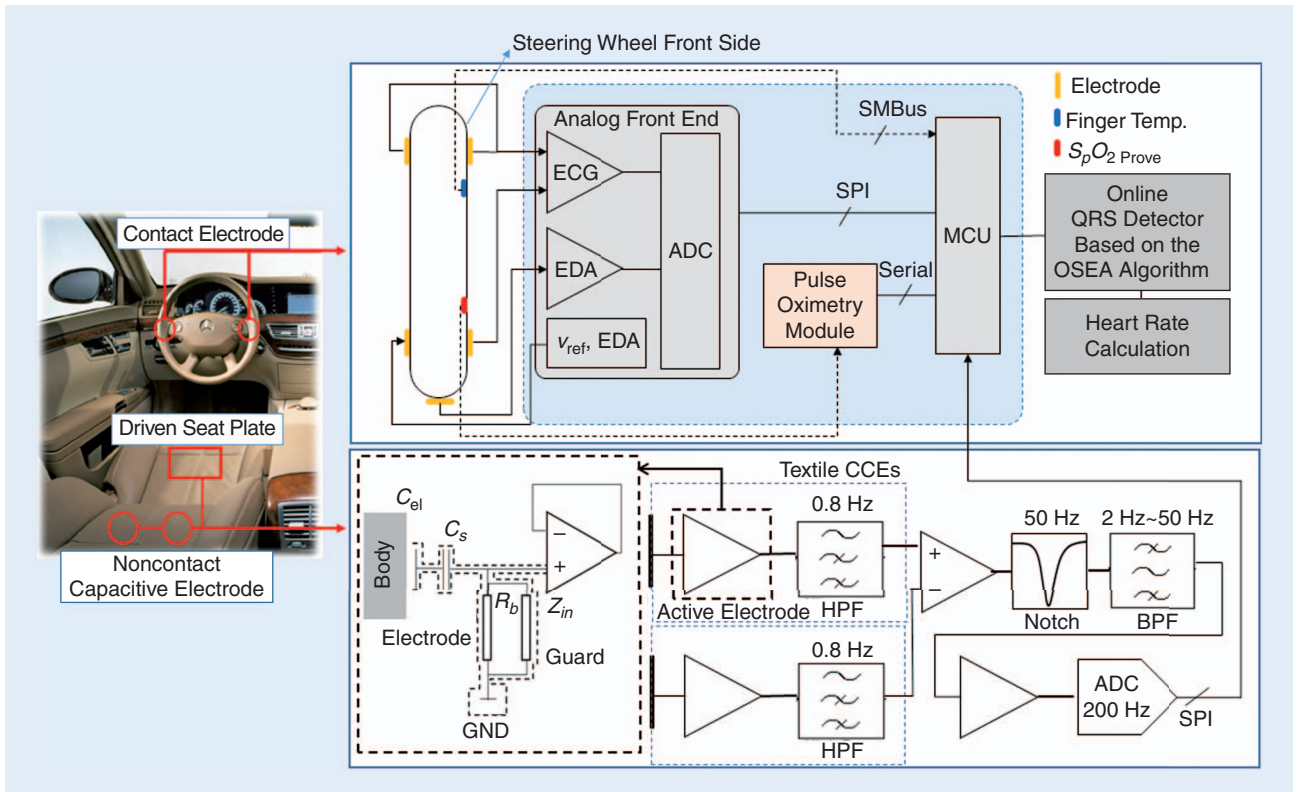


FIGURE 5. Analog signal processing for ECG acquisition technique by Daimler AG [10], [31].

to the steering wheel for a contact-based ECG acquisition, while capacitively coupled electrodes are attached to the seat and on the backrest of the seat for a noncontact-based ECG acquisition. Daimler AG employs an active electrode technique to get a high input impedance, similarly to the study by Ford. In the study [10], [31], Daimler AG can successfully reduce the variation of the capacitance between the driver and electrodes by connecting a capacitor ( $C_s$ ) to an amplifier input in series [31]. An HPF ( $f_c = 0.8$  Hz) is applied to the analog front end to reduce a baseline drift and dc offsets. Noise generated from the power baseline is removed by a notch filter ( $f_c = 50$  Hz) and a bandpass filter ( $f_{cl} = 2$  Hz and  $f_{ch} = 50$  Hz).

### DSM algorithms processing physiological signals

The DSM systems utilizing physiological signals need to remove artifacts in the signal measurements and to detect a driver's status while driving [5]. Therefore, DSM algorithms focus on removing artifacts, but there are few studies introduced in the literature. This section introduces DSM algorithms for contact-based ECG acquisition and noncontact-based ECG acquisition techniques developed by Toyota and Ford, respectively.

The signal detection function in the Toyota's DSM algorithm [8] calculates the correlation coefficient  $r$  successively by matching the QRS complex candidate found in the signal measurements with a QRS complex template. When  $r$  is larger than the threshold 0.7, the prompt QRS complex candidate is assumed a true QRS complex, as explained in the

QRS detection in Figure 6(a). The RR interval is measured between the two consecutive QRS complexes, and stored in the RR interval vector  $\vec{I}$ . Note that the detected R-peak positions are used to measure the RR intervals, however, there are true R-peaks and false R-peaks (outlier) due to the motion artifacts by the driver in the detected R-peaks.

The signal enhancement function in Figure 6(b) is performed to eliminate the R-peak by motion artifacts in the following steps:

- Calculate the mean ( $\mu_{\vec{I}}$ ) and the standard deviation ( $\sigma_{\vec{I}}$ ) of  $\vec{I}$ .
- Exclude outliers and store the RR intervals remaining after the exclusion of outliers to  $\vec{J}$ .
- Calculate the standard deviation ( $\sigma_{\vec{J}}$ ) and the median (Med  $\vec{J}$ ) of  $\vec{J}$  of a set of 11 consecutive intervals in  $\vec{J}$  for each time index.
- Search for and remove outliers using the Med  $\vec{J}$  and  $\sigma_{\vec{J}}$ .
- Calculate the smoothed RR interval ( $\overline{\text{RRI}}$ ) by replacing the detected outliers with Med  $\vec{J}$ .

The driver status analysis function in Figure 6(c) consists of signal analysis and detection rules subfunctions. In the signal analysis subfunction,  $\overline{\text{RRI}}$  is transformed into the frequency domain to find the frequency parameter that is related to the sympathetic and parasympathetic nerves using the following steps:

- Sample  $\overline{\text{RRI}}$  at 8 Hz.
- Divide sampled  $\overline{\text{RRI}}$  data in five epoch intervals to obtain confident spectral estimation and to apply



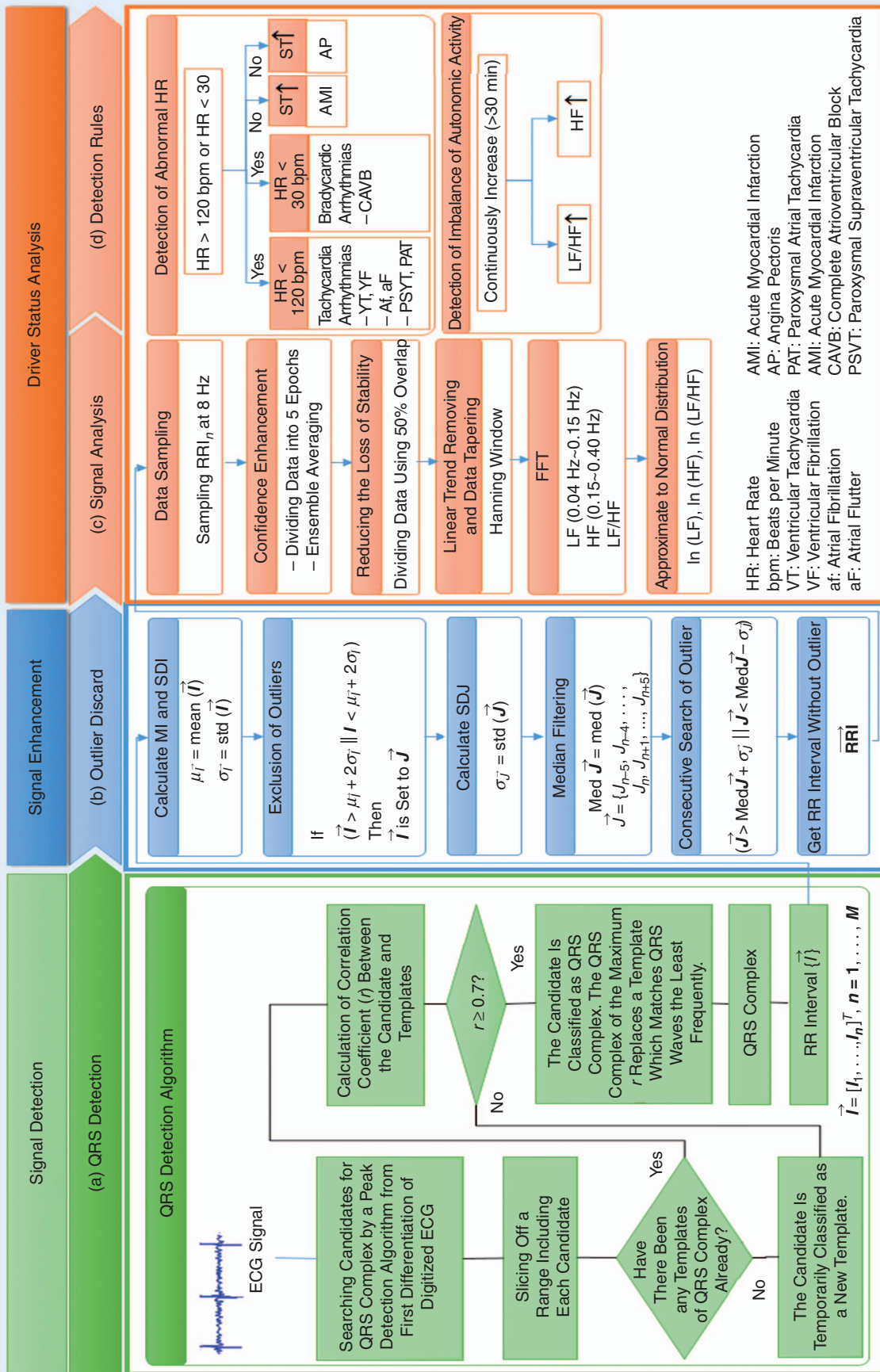


**FIGURE 6.** Toyota's DSM algorithm.

ensemble averaging, where the data length of each epoch is 64 seconds. The data is divided using 50% overlap to reduce the loss of stability.

- Apply the Hanning window to reduce linear trends in the data.
- Calculate the power of LF components that is a parameter of combined sympathetic and parasympathetic activities, the power of HF components that is a parameter of parasympathetic activity, and the ratio LF/HF as a parameter of sympathetic activity for each epoch.
- Calculate the natural logarithms of LF, HF, and LF/HF to approximate the distributions of LF, HF, and LF/HF to the normal distribution.

Toyota attached a chest ECG detection patch directly to the driver's chest [8], [19] to compare the ECG obtained from the patch with that measured from the DSM system. The mutual information technique (MIT) [8], which measures the similarity between two signals, is used to compare the two ECGs. The value of MIT higher than 0.047 indicates that two signals are strongly correlated, and in Toyota's study [19], the MIT value of the two ECGs is much higher than 0.047; MIT values for HR,  $\ln(\text{LF})$ ,  $\ln(\text{HF})$ , and  $\ln(\text{LF}/\text{HF})$  are 0.225, 0.223, 0.209, 0.184, respectively, with 95% confidence interval.

When the measured ECG includes too many R-peaks with motion artifacts, it is impossible to continuously detect the R-peaks successfully. Therefore, in practice, PPG is acquired to detect the lost RR intervals in the ECG so that the missing RR intervals can be replaced with the PPG peak intervals.

The detection rules subfunction analyzes the status of the driver using the  $\ln(\text{LF})$ ,  $\ln(\text{HF})$ , and  $\ln(\text{LF}/\text{HF})$  calculated in the signal analysis subfunction and the HR obtained from RR intervals [8], [19]. As explained in Figure 6(d), Toyota defines the detection rule of abnormal physiological status based on the HR, and demonstrates that the driver is drowsy if the LF/HF or HF increases steadily for more than 30 minutes.

Ford introduces another DSM algorithm utilizing a signal processing technique to remove outliers [16] and the HRV technique [7] to detect the driver workload. QRS complex is extracted from ECG by open source ECG analysis (OSEA) [32] as described in Figure 7(a), and the outliers of the extracted QRS complex are removed as explained in Figure 7(b)–(d). In the algorithm, a signal enhancement function using the quality indices  $QI$  is applied [16]. The basic quality indices used in the algorithm are quality index amplitude ( $QI_{\text{Amplitude}}$ ), quality index standard deviation ( $QI_{\text{Std}}$ ), and quality index saturation ( $QI_{\text{sat}}$ ), as defined in Figure 7(b), that are calculated using  $\vec{x}_m$  and  $\vec{x}_{m,\text{in}}$ , where  $\vec{x}_m$  and  $\vec{x}_{m,\text{in}}$  are the vectors of the signal measurements within  $\pm 200$  milliseconds and  $\pm 50$  milliseconds around the prompt R-peak of the QRS complex, respectively. The quality index amplitude  $QI_{\text{Amplitude}}$  is the peak-to-peak amplitude ratio of  $\vec{x}_{m,\text{in}}$  and

$\vec{x}_m$  and used to discard strong but short baseline shift in  $\vec{x}_m$ ,  $QI_{\text{Std}}$  is the standard deviation ratio of  $\vec{x}_{m,\text{in}}$  and  $\vec{x}_m$ , and  $QI_{\text{Std},m}$  indicates how much the R-peak of  $\vec{x}_m$  is separated from the noise around the R-peak. The quality index saturation  $QI_{\text{sat}}$  is a binary-valued index used to detect samples, in  $\vec{x}_m$ , that belong to the upper or lower saturation region of the ECG amplifier. The quality indices multiplication  $QI_m$  is calculated by multiplying  $QI_{\text{Amplitude}}$ ,  $QI_{\text{Std}}$ , and  $QI_{\text{sat}}$ , and is used to remove outliers and to generate a training data before applying to the principal component analysis (PCA). The PCA and Hotelling's T-squared value [16] are used to calculate the probabilistic distance from the QRS complex to the center of the training data, and to calculate the confidence measure (CM). A vector with a small deviation to the training data will result in a small Hotelling's T-squared value and, hence, is very likely to be a true QRS complex [16].

Since Ford's noncontact-based ECG acquisition technique measures the ECGs from multiple pairs of electrodes, the peaks from different channels need to be aligned before evaluating each QRS complex.

Referring to the ANSI/AAMI EC 57 norm

[32], all R-peaks from the multiple [three in Figure 7(d)] channels within a time interval of  $\pm 75$  ms can be assumed one single R-peak from the same heartbeat, and a missing R-peak in a channel is removed for the later processing. This leads to triplets of CMs based on Hotelling's T-squared values. The number of CMs whose values are smaller than a specific threshold determines if the R-peak is from a true QRS complex [16].

In [7], Ford found the relationship between the driver's HR and driver workload from the real driving tests. In the study, two men and two women (average age of  $29.5 \pm 2.08$  years) are selected as the subjects, and the authors collected the ECGs while driving between Aachen and Brussels. The analysis of the driver's status is performed in both time and frequency domains. This study proves that the driver's HR and driver workload have a strong relationship, as shown in Figure 7(e), while the percentage of the power in the LF segments,  $LF_{AR}[\%]$ , is not very related to the driver workload. In particular, the HRs of all subjects are about 75~86 beats/minute in the city, about 72~83 beats/minute on highway I, and about 68~84 beats/minute on highway II. The traffic congestion in the city results in a higher HR, which indicates that the driver workload in the city is greater than that on the highway.

## EMC issues in DSM systems using physiological signals

As the smart vehicles offer more driver-friendly functions, the number of electrical control units (ECUs) is growing. As a result, the number of problems caused by the electromagnetic waves from the ECUs is continuously increasing. Since the physiological signals, such as ECG, that is typically around  $100\mu\text{V}\sim 3\text{mV}$  are very sensitive to electromagnetic waves, it

**It is essential to design an analog signal processing circuit with a consideration of EMC to protect the DSM system from noise and interference from the ECUs.**

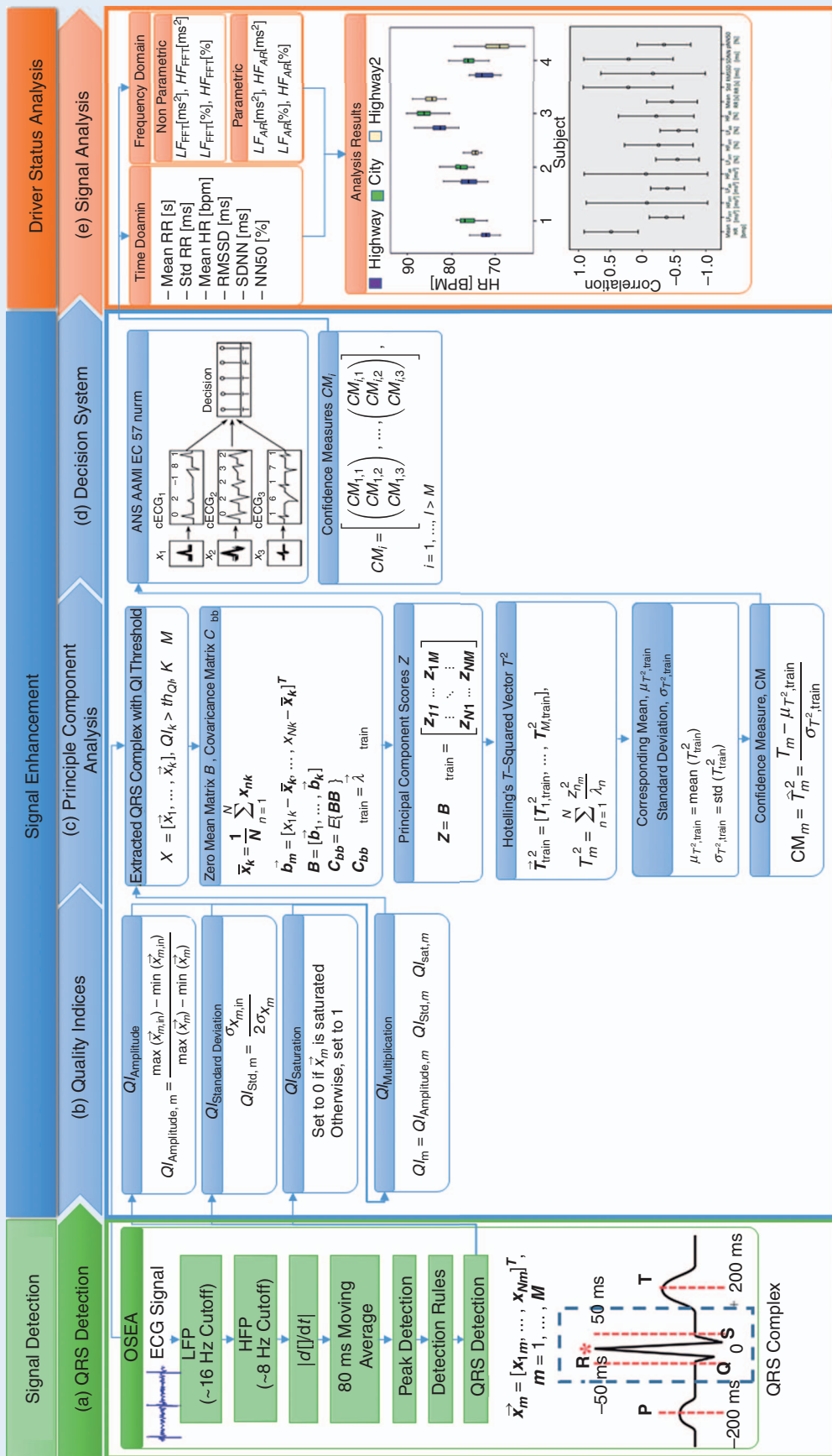


**FIGURE 7.** Ford's DSM algorithm.



may cause a malfunction of the DSM system. Therefore, it is essential to design an analog signal processing circuit with a consideration of EMC to protect the DSM system from noise and interference from the ECUs.

Therefore, in this section, we investigate the four EMCs, i.e., electromagnetic interference (EMI), electromagnetic susceptibility (EMS), surge, electrostatic discharge (ESD), that need to be considered when applying a DSM system using physiological signals to the vehicles.

EMI is the electromagnetic wave emitted from the ECU. As the electromagnetic waves can cause errors in other electronic devices, ECUs should be designed not to emit electromagnetic waves over the levels approved by the standard. In general, EMI is classified into conducted emission (CE) and radiated emission (RE);

CE is the electromagnetic noise that is generated at frequencies of 30 MHz or lower from an ECU and penetrates into other ECUs through signal lines and power lines. Meanwhile, RE is the electromagnetic noise that is created at frequencies of 30 MHz or higher and propagates through the air.

The EMS indicates the impact of electromagnetic interference from outside a vehicle. EMS is classified into bulk current injection (BCI) and radiated susceptibility (RS). BCI is defined as the endurance of electromagnetic interference released through power connectors, while RS is the endurance of electromagnetic interference transmitted through the air. Therefore, in particular, the noise floor of the DSM systems for HR monitoring should be set to satisfy a noise level equivalent to 25  $\mu\text{V}$  peak to peak over the bandwidth of 0.5–40 Hz [34].

A surge noise occurs when a sudden voltage is applied or current change occurs, for example, turning on/off of adjacent ECUs. This may supply a large current or voltage to the DSM system instantaneously. In general, a human's heart is the most sensitive to an electric current in a frequency range between 50–60 Hz so that a small current of 35  $\mu\text{A}$  root mean square (rms) can damage the heart and cause a life-threatening event. Therefore, the DSM systems using the ECG should be carefully designed by employing a resistance or current limiting to allow a current of less than 10  $\mu\text{A}$  rms to flow through the system [34].

Electrostatic discharge (ESD) is the sudden flow of electricity between two electrically charged objects by contact; it occurs when the driver touches the electrodes. The DSM system needs to limit the current that can be discharged through the contact of the driver's hand, so it requires a built-in protection circuitry to mitigate the ESD [34].

As a result, the DSM systems using physiological signals must be tested based on EMC standards. The EMC tests should be conducted with the CISPR (International Special Committee on Radio Interference) standards for emissions and the International Organization for Standardization (ISO) standards for susceptibility. EMI, EMS, surge noise, and ESD are

assessed by the CISPR25, ISO11452, ISO7637, and ISO10605 standards, respectively.

## Conclusions

Traffic accidents are one of the most serious problems threatening the safety of automobile users. As reported in [4], the driver's incapacitation due to drowsiness and fatigue is one of the major causes resulting in fatal traffic accidents. The DSM system is an innovative solution that can dramatically reduce traffic accidents caused by the driver's incapacitation [35]. Therefore, it is essential to develop DSM systems using vision sensors and SASS or using the driver's physiological signals such as ECG or PPG. The DSM systems using physiological signals have recently been developed by automo-

bile manufacturers because physiological signals contain an accurate information of the HR, which is very useful to determine the driver's physical status. In this study, we have introduced analog signal processing techniques employed in the DSM systems to acquire the physiological signals and DSM algorithms to detect the driver's status. However, DSM systems using physiological signals require further research on analog signal processing techniques, since physiological signals are very weak and vulnerable to noise and interference in the in-vehicle environments. Studies have shown that automobile manufacturers, universities, and research institutions are making efforts to improve the performance of the DSM systems using physiological signals and to apply the system to real vehicles. We expect that employing the DSM system will reduce traffic accidents due to the driver's incapacitation and, therefore, enhance the safety of automobile users.

## Acknowledgments

Seung-Hyun Kong is the corresponding author of this article. This work (2013R1A2A2A01067863) was supported by the Midcareer Researcher Program through a National Research Foundation grant funded by the Korean government (MEST).

## Authors

**Youjun Choi** (uchoi@kaist.ac.kr) received his B.S. degree in electrical engineering from Chonbuk National University in 2006, his M.S. degree in mechatronics engineering from the Gwangju Institute of Science and Technology in 2008, and he is currently a Ph.D. candidate with the Cho Chun Shik Graduate School for Green Transportation at the Korea Advanced Institute of Science and Technology, South Korea. Since 2011, he has been a senior researcher at the Korea Automotive Technology Institute. His research interests include mobility integration service and driver status monitoring systems for automotive.

**Sang Ik Han** (sangik.han@kaist.ac.kr) received his B.S. degree in electrical and electronics engineering from

**The DSM system is an innovative solution that can dramatically reduce traffic accidents caused by the driver's incapacitation.**

Chung-Ang University, Seoul, South Korea, in 2006; his M.S. degree in optics from the University of Central Florida, Orlando, in 2009; and his Ph.D. degree in electrical engineering from the University of Texas at Dallas, Richardson, in 2014. He is currently a research associate with the Cho Chun Shik Graduate School for Green Transportation at the Korea Advanced Institute of Science and Technology, South Korea.

**Seung-Hyun Kong** (skong@kaist.ac.kr) received his B.S. degree in electronics engineering from Sogang University, Seoul, South Korea, in 1992; his M.S. degree in electrical and computer engineering from Polytechnic University, New York, in 1994; and his Ph.D. degree in aeronautics and astronautics from Stanford University, Palo Alto, California, in 2005. His research interests include vehicular localization and navigation techniques, vehicular communication systems, cooperative vehicle systems, and advanced signal processing techniques for sensors and vehicular applications. He is currently an associate professor in the Cho Chun Shik Graduate School for Green Transportation at the Korea Advanced Institute of Science and Technology, South Korea, where he has been a faculty member since 2010. He is a Senior Member of the IEEE.

**Hyunwoo Ko** (kohyunwoo@kaist.ac.kr) received his B.S. degree in mechanical and control engineering from Handong Global University, Pohang, in 2014, and his M.S. degree from the Cho Chun Shik Graduate School for Green Transportation at the Korea Advanced Institute of Science and Technology, Daejeon, South Korea, in 2016.

## References

- [1] S. C. Davis, S. W. Diegel, and R. G. Boundy, "Transportation Energy Data Book: Edition 34," Office of Energy Efficiency and Renewable, Oak Ridge National Laboratory, report ORNL-6991, 2015.
- [2] J. C. Fell and M. Freedman, "The relative frequency of unsafe driving acts in serious traffic crashes," National Highway Traffic Safety Administration (NHTSA), report DOT-HS-809-206, Washington, DC, 2001.
- [3] B. C. Tefft, "Prevalence of motor vehicle crashes involving drowsy drivers, United States, 2009–2013," Report Prepared for the American Automobile Association (AAA) Foundation for Traffic Safety, Washington, DC, 2014.
- [4] T. Akerstedt, C. Bassetti, F. Cirignotta, D. Garcia-borreguero, M. Goncalves, J. Horne, D. Leger, M. Partinen, T. Penzel, P. Philip, and J. C. Verster, "Sleepiness at the wheel," Institut National du Sommeil et de la Vigilance, European Sleep Research Society, 2013.
- [5] Y. Dong, Z. Hu, K. Uchimura, and N. Murayama, "Driver inattention monitoring system for intelligent vehicles: A review," *IEEE Trans. Intell. Transp. Syst.*, vol. 12, no. 2, pp. 596–614, 2011.
- [6] S. Boverie, "General driver monitoring module definition SoA," Public Rep. DESERVE No. D3.2.1, 2013.
- [7] B. Eilebrecht, S. Wolter, J. Lem, H. J. Lindner, R. Vogt, M. Malter, and S. Leonhardt, "The relevance of HRV parameters for driver workload detection in real world driving," presented at the IEEE Computing in Cardiology Conf., Krakow, Poland, Sept. 2012.
- [8] M. Osaka. (2012). Customized heart check system by using integrated information of electrocardiogram and plethysmogram outside the driver's awareness from an automobile steering wheel [Online]. INTECH Open Access Publisher. Available: <http://cdn.intechopen.com/pdfs-wm/27021.pdf>
- [9] L. D'Angelo and T. C. Luth, "Integrated systems for distraction-free vital signs measurement in vehicles," *ATZ Worldwide eMag.*, vol. 113, no. 11, pp. 52–56, 2011.
- [10] L. T. D'Angelo, J. Parlow, W. Spiessl, S. Hoch, and T. C. Luth, "A system for unobtrusive in-car vital parameter acquisition and processing," presented at the 4th Int. Conf. IEEE Pervasive Computing Technologies for Healthcare, Munich, Mar. 2010.
- [11] S. Heuer, B. Chamadiya, A. Gharbi, C. Kunze, and M. Wagner, "Unobtrusive in-vehicle biosignal instrumentation for advanced driver assistance and active safety," presented at the IEEE EMBS Conf., Kuala Lumpur, Malaysia, 2010.
- [12] Mercedes-Benz. (2016). Attention assist system [Online]. Available: [https://techcenter.mercedes-benz.com/en\\_CA/attention\\_assist/detail.html](https://techcenter.mercedes-benz.com/en_CA/attention_assist/detail.html)
- [13] T. Von Jan, T. Karnahl, K. Seifert, J. Hilgenstock, and R. Zobel, "Don't sleep and drive-VW's fatigue detection technology," in *Proc. 19th Int. Conf. Enhanced Safety of Vehicles*, 2005, pp. 1–12.
- [14] Volvo Technology Corp., "Method for interpreting a drivers' head and eye activity," Eur. Patent EP2204118B1, July 23, 2014.
- [15] M. Walter, B. Eilebrecht, T. Wartzek, and S. Leonhardt, "The smart car seat: Personalized monitoring of vital signs in automotive applications," *Pers. Ubiquit. Comput.*, vol. 15, no. 7, pp. 707–715, 2011.
- [16] T. Wartzek, B. Eilebrecht, J. Lem, H.-J. Linder, S. Leonhardt, and M. Walter, "ECG on the road: Robust and unobtrusive estimation of heart rate," *IEEE Trans. Biomed. Eng.*, vol. 58, no. 11, pp. 3112–3120, 2011.
- [17] K. Futatsuyama, T. Kawachi, and T. Nakagawa, "Cuffless blood pressure monitoring using steering wheel sensor system," *Trans. Jpn. Soc. Med. Biol. Eng.*, vol. 52, Supplement, pp. OS-67–OS-68, Oct. 2014.
- [18] K. Futatsuyama, N. Mitsumoto, T. Kawachi, and T. Nakagawa, "Noise robust optical sensor for driver's vital signs," SAE Technical Paper 2011-01-1024, 2011, doi:10.4271/2011-01-1024.
- [19] M. Osaka, H. Murata, Y. Fuwamoto, S. Nanba, K. Sakai, and T. Katoh, "Application of heart rate variability analysis to electrocardiogram recorded outside the driver's awareness from an automobile steering wheel," *Circulation J.*, vol. 72, no. 11, pp. 1867–1873, 2008.
- [20] K. Sakai, K. Yanai, S. Okada, and K. Nishii, "Design of seat mounted ECG sensor system for vehicle application," *SAE Int. J. Passeng. Cars-Electron. Electr. Syst.* 6(1):342–348, 2013, doi:10.4271/2013-01-1339.
- [21] Nissan Motor Co. Ltd., "Driver's fatigue degree estimation apparatus and driver's fatigue degree estimation method," U.S. Patent 0 164 400 A1, June 18, 2015.
- [22] M. Elgendi, B. Eskofier, S. Dokos, and D. Abbott, "Revisiting QRS detection methodologies for portable, wearable, battery-operated, and wireless ECG systems," *PLoS One*, vol. 9, no. 1, pp. e845101, 2014.
- [23] P. E. McSharry, G. D. Clifford, L. Tarassenko, and L. A. Smith, "A dynamical model for generating synthetic electrocardiogram signals," *IEEE Trans. Biomed. Eng.*, vol. 50, no. 3, pp. 289–294, 2003.
- [24] D. McDuff, S. Gontarek, and R. W. Picard, "Remote detection of photoplethysmographic systolic and diastolic peaks using a digital camera," *IEEE Trans. Biomed. Eng.*, vol. 61, no. 12, pp. 2948–2954, 2014.
- [25] B. Kim, S.-H. Kong, and S. Kim, "Low computational enhancement of STFT-based parameter estimation," *IEEE J. Select. Topics Signal Process.*, vol. 9, no. 8, pp. 1610–1619, 2015.
- [26] M. Z. Poh, N. C. Swenson, and R. W. Picard, "A wearable sensor for unobtrusive, long-term assessment of electrodermal activity," *IEEE Trans. Biomed. Eng.*, vol. 57, no. 5, pp. 1243–1252, 2010.
- [27] B. Winter Bruce and J. G. Webster, "Driven-right-leg circuit design," *IEEE Trans. Biomed. Eng.*, vol. BME-30, no. 1, pp. 62–6, Jan. 1983.
- [28] S. Leonhardt and A. Aleksandrivic, "Non-contact ECG monitoring for automotive application," in *Proc. 5th Int. Symp. Medical Devices and Biosensors*, Hong Kong, China, 2008, pp. 183–185.
- [29] R. J. Prance, A. Debray, T. D. Clark, H. Prance, M. Nock, C. J. Harland, and A. J. Clippingdale, "An ultra-low-noise electrical-potential probe for human-body scanning," *Meas. Sci. Technol.*, vol. 11, no. 3, pp. 291–297, 2000.
- [30] A. Schommartz, B. Eilbrecht, T. Wartzek, M. Walter, and S. Leonhardt, "Advances in modern capacitive ECG systems for continuous cardiovascular monitoring," *Acta Polytech.*, vol. 51, no. 5, pp. 100–105, 2011.
- [31] B. Chamadiya, S. Heuer, U. G. Hofmann, and M. Wagner, "Towards a capacitively coupled electrocardiography system for car seat integration," in *Proc. 4th European Conf. Int. Federation for Medical and Biological Engineering*, Berlin, Germany, 2009, vol. 22, pp. 1217–1221.
- [32] P. Hamilton, "Open source ECG analysis," in *Proc. IEEE Computers in Cardiology Conf.*, 2002, pp. 101–104.
- [33] "Testing and reporting performance results of cardiac rhythm and ST segment measurement algorithms," ANSI/Association for the Advancement of Medical Instrumentation, Tech. Rep. EC57, 1998.
- [34] B. Crone, "Mitigation strategies for ECG design challenges," Analog Devices Inc., Tech. Rep. MS-2160, 2011.
- [35] I. Akahashi, T. N. H. Kanamori, T. Tanaka, S. Kato, Y. Ninomiya, E. Takeuchi, M. Makiguchi, and H. Aoki, "Automated safety vehicle stop system for cardiac emergencies," presented at the IEEE Int. Conf. Emerging Technologies and Innovative Business Practices for the Transformation of Societies, Balacava, Mauritius, 2016.